Millimeter-Wave Radar Phenomenology of Power Lines and a Polarimetric Detection Algorithm

Kamal Sarabandi, *Fellow, IEEE*, and Moonsoo Park

***Abstract*— In this paper, the radar phenomenology of high-voltage power lines and cables is studied for examining the feasibility of detecting power lines along the path of a low-flying aircraft using a millimeter-wave radar system. For this purpose, polarimetric backscatter measurements of power line samples of different diameters and strand arrangements were performed over a wide range of incidence angles with very fine increments at 94 GHz. Also, similar polarimetric backscatter measurements were conducted for cylinders of the same radii and lengths as the power line samples for identifying the scattering features caused by the braiding structure of the power lines. In addition, the effects of a thin layer of water and a layer of ice over the power line surface on its polarimetric scattering behavior are studied by repeating the polarimetric backscatter measurements. Based on this phenomenological study, a polarimetric detection algorithm that makes use of the scattering features caused by the braided structure of power lines is proposed. It is shown that the proposed algorithm is capable of detecting power lines in a relatively strong clutter background with a poor signal-to-clutter ratio. The performance of the algorithm is demonstrated experimentally using a rough asphalt surface and a vegetation foliage as sample clutter backgrounds.**

***Index Terms*—Power lines, radar polarimetry.**

I. Introduction

HIGH-voltage power lines and their supporting towers create hazardous conditions for low-flying aircrafts and helicopters. Army aviation and other services have an urgent need for an automated system to alarm pilots of the existence, direction, and the distance of nearby cables. In the past, a number of approaches including millimeter-wave radars have been proposed for detecting power lines [1]–[4]. An electro-optical laser approach is currently being pursued as a solution to this problem. Despite many advantages offered by such system including fine resolution and compactness, there are a number of major limitations including: 1) limited range; 2) significant atmospheric attenuation under inclement weather conditions; and 3) limited ability to automate the wire detection warning for pilots. As a result of these limitations, the laser systems have not preceded beyond the technology demonstration phase. Like electro-optical laser systems, relatively compact radar systems can be constructed at millimeter-wave frequencies, however, their performance are not limited by bad weather conditions. In this paper, the feasibility of power line detection using millimeter-wave radars is revisited. In [3], it is concluded that since significant backscatter exists only over narrow aspect angles near normal incidence at discrete Bragg directions, it is not possible to detect power lines with a high probability, especially in the presence of background clutter.

It is true that in a real radar environment, the presence of clutter may increase the false alarm rate to an extent which would impair target detectability. Radar polarimetry is usually used to improve the probability of detection and to reduce the false alarm rate [6]. For distinguishing a target in background clutter, structure dependent polarimetric features of the target must be characterized and employed in target detection. Power lines are made of strands of wires in helical arrangement and this can be exploited for detecting the power lines in a clutter background. At high frequencies, the effects of helicity and periodicity of power line surface features become important factors in the scattering behavior of power lines. Existence of cross-polarized component in the radar backscatter usually provides a unique target signature. Because of tilted grooves on the power line surface that can support corner reflector type multiple reflection, it is expected that a considerable cross-polarized backscatter will be generated. These effects are investigated in more details in this paper based on which a polarimetric detection algorithm is developed.

Four different power line samples of different diameters and strand arrangement were chosen and their backscatter responses were measured and compared with those of metallic cylinders having length and diameters identical to the length and diameters of the power line samples. Backscatter behavior of wet and frozen power lines are also reported to demonstrate the effect of a thin layer of water and ice on the polarimetric response of power lines. The polarimetric detection algorithm developed in this investigation is based on the expected coherence relation between the copolarized and cross-polarized backscatter component of power lines which allows target detection under a poor signal-to-clutter ratio. To examine the degree of coherence between the copolarized and cross-polarized backscatter, histograms of backscatter measurements at different aspect angles, were obtained by moving the antenna footprint along the power lines and by

Manuscript received September 21, 1998; revised August 31, 1999. This work was supported by the U.S. Army Research Laboratory under Cooperative Agreement DAAL01-96-2-0001 and prepared through collaborative participation in the Advanced Sensors Consortium. It was also supported by the U.S. Army Research Laboratory under Cooperative Agreement DAAL01-96-2-0001.

The authors are with the Radiation Laboratory, Department of Electrical Engineering and Computer Science, The University of Michigan, Ann Arbor, MI 48109-2122 USA.

Publisher Item Identifier S 0018-926X(99)09982-2.

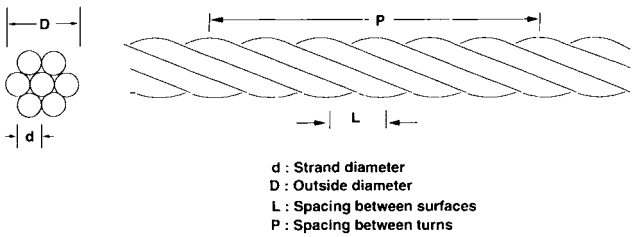

Fig. 1. Geometry and important structural parameters of a power line.

rotating the power lines about their axes. Finally, the success of the detection algorithm is tested by measuring the backscatter from a power line in the presence of a strong backscatter clutter.

II. Experimental Setup

Polarimetric backscatter measurements of the power line samples were performed at 94 GHz using the University of Michigan millimeter-wave fully polarimetric radar system. This radar is a stepped frequency radar capable of transmitting a linear chirped signal with a bandwidth of 1 GHz and can be operated either in coherent or coherent-on-receive modes [2]. For the measured results reported in this study, the coherent mode was used. Significant isolation between the transmit and receive channels are achieved using two separate antennas for the transmitter and receiver. However, the transmitter antenna has a wider beamwidth to minimize parallax problem and the targets are positioned far enough from the radar so that the radar measurements are nearly in the backscatter direction. The block diagram of the measurement setup for collecting polarimetric radar cross section (RCS) data is shown in Fig. 2. The core of the system is an HP-8753C vector network analyzer with both phase and amplitude measurement capability and a 100 dB dynamic range. The ability of the network analyzer to generate the time-domain response from the frequency response allows removal of unwanted signals from the desired target response. To measure the backscatter response of the power line samples with high signal to background ratio for all incident angles, the power lines were mounted on a U-shape styrofoam structure, which is designed for very low radar backscatter response at the target range. The polarimetric radar cross section of the mount was measured for the angular range 0° to 50°. It was observed that the RCS level of the mount never exceeded -45 [dBsm] for all polarizations and aspect angles. To further reduce the backscatter from the mounting structure, the backscatter from the mount was coherently subtracted from that of the target and the mount. To facilitate backscatter measurement at different incident angles a precision computer controlled turntable with an accuracy of a fraction of a tenth of a degree was used.

One important issue in polarimetric RCS measurements is the calibration. In this procedure, the systematic errors, such as channel imbalances and antenna crosstalks are removed and the data is radiometrically scaled. The measured polarimetric data are calibrated using a 7.6-cm metallic sphere and a depolarizing target according to the procedure outlined in [2]. It should be noted here that since power lines are targets of

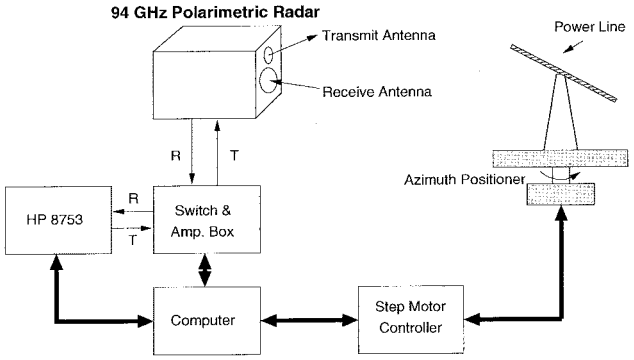

Fig. 2. Measurement setup.

TABLE I
Geometrical Specifications of the Power Lines

No.	Al/Copper		Steel		D [cm]	P [cm]	L [cm]
	# of St.	d [cm]	# of St.	d [cm]			
1	7	0.400	-	-	1.20	14.60	1.95
2	19	0.446	-	-	2.22	23.5	1.52
3	54	0.337	7	0.337	3.01	35.56	2.00
4	45	0.446	7	0.301	3.52	40.65	2.40

infinite extent (their length are usually larger than the antenna footprint) radiometric calibration is not well defined because of the magnitude and phase variation of the antenna footprint over the target. Hence, the absolute radiometric calibration is not possible and the measurements are system dependent. The RCS values reported in this paper are obtained assuming the power line is a point target located at the antenna boresight. The accuracy of the calibration technique has been determined to be ± 0.5 dB in magnitude and $\pm 5°$ in phase [2]. To ensure the accuracy of the measured results the calibration procedure was performed at the beginning and at the end of each power line measurement.

Backscatter response of a power line is mainly characterized by the size and arrangement of the outer layer of the constituent strands. Four typical power line samples were selected. Fig. 1 shows the geometry of a typical power line. The conducting wires are wound around a core in a helical fashion forming a periodic structure. It should be noted that the periodicity of the structure is smaller than the pitch of the helix and depends on the number of strands on the outer layer. The structural information and dimensions of the four different power lines used in these experiments are listed in Table I. The diameters of the power lines range from 1.2 to 3.52 cm and their strand diameters vary from 0.34 to 0.45 cm. As is shown in Table I, the surface period of these power lines, varying from 1.2 to 3.52 cm, depends on the pitch, strand diameter, and the number of strands on the outer layer. The power lines used in the RCS measurements were about 1 m long positioned at about 12 m from the radar system. The half-power beamwidth (HPBW) of this radar is 1.4° producing a footprint of about 30 cm at the target position. The cable lengths and the target distance are chosen so that there is no considerable radar backscatter from the power lines ends.

The targets were positioned in the horizontal plane and their radar backscatter responses were measured in the radar

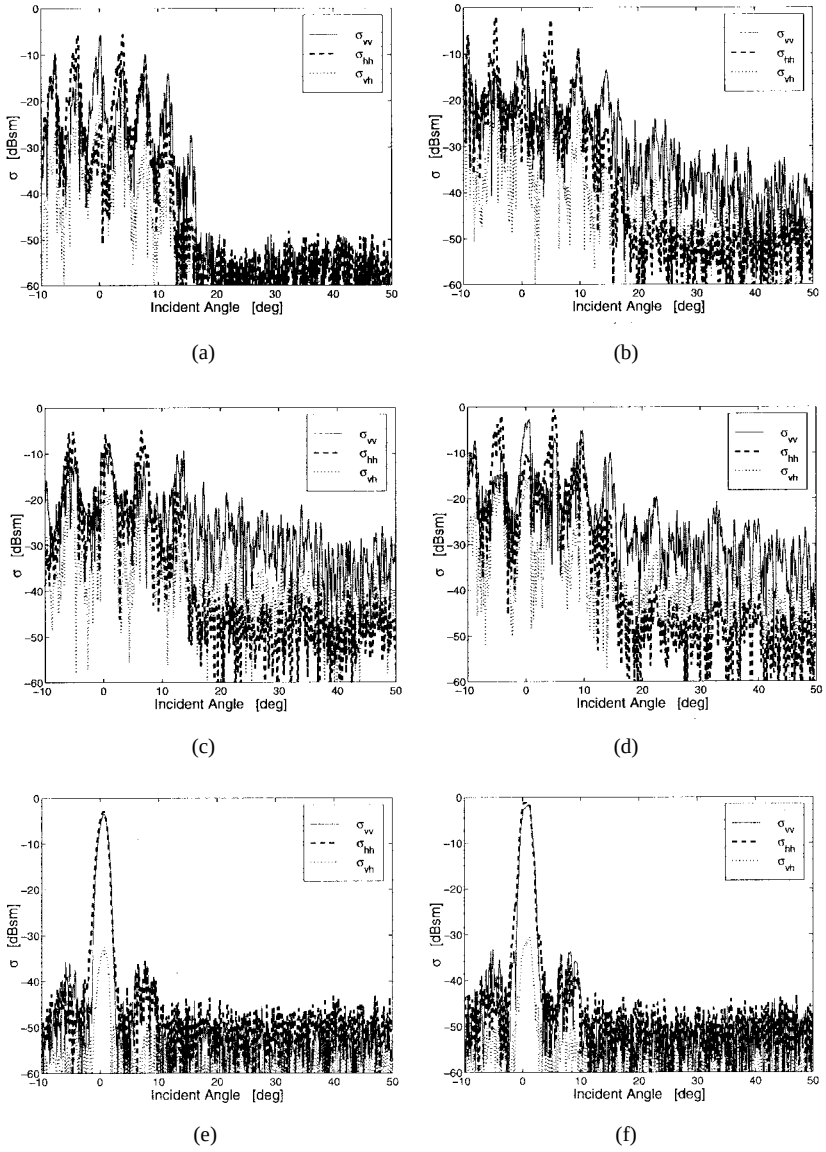

Fig. 3. Polarimetric backscatter responses of the four power line samples used in this study and two cylinder counterpart of power line #1 and #2. (a) Power line #1. (b) Power line #2. (c) Power line #3. (d) Power line #4. (e) Cylinder #1. (f) Cylinder #2.

antenna principal plane. This configuration is similar to that of a radar system on low-flying aircraft heading toward a power line in the horizontal plane. Angular RCS measurements were performed by rotating power lines in the principal plane. In cases where the power line is not in the principal plane, circular symmetry of the power line can be used to obtain the scattering matrix of the power line from those measured in the principal plane [1].

In addition to power line samples, the radar backscatter responses of four smooth metallic cylinders having lengths and diameters identical to those of the power lines were measured to identify the effects of braiding on the polarimetric backscatter response. The power lines and cylinders were measured over the angular range -10° to 50° with a fine angular resolution (steps of 0.1°). To reduce the noise floor of the system, eight traces at each target position were acquired and averaged coherently. The backscatter measurement for each power line was repeated to ensure measurement consistency.

III. Experimental Results

In this section, a summary of the polarimetric backscatter behavior of power lines is given. As mentioned earlier, backscatter of the power line samples were determined experimentally under three surface conditions: dry, wet, and frozen. Fig. 3(a)–(f) shows the polarimetric radar backscatter responses of the four power lines and two smooth cylinders under dry conditions. Comparing Fig. 3(a) and (b) with Fig. 3(e) and f), significant differences between the backscatter response of power lines and their counterpart smooth cylinders are seen. Cylinder backscatter exists only at normal incidence and no cross-polarized backscatter is generated whereas power lines generate considerable backscatter in all polarizations and over a wide range of incidence angles. Strong backscatter peaks occur at normal incidence and at certain discrete incidence angles. These peaks are known as Bragg modes in the backscatter direction caused by the constructive interference of backscatter

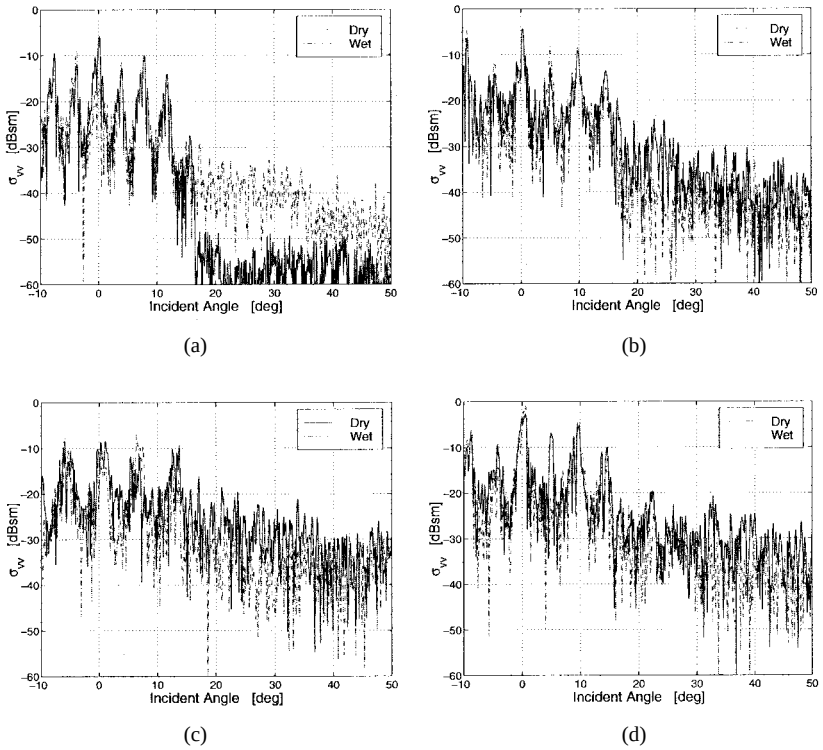

Fig. 4. Vertical (VV)-polarized backscatter responses of the four power line samples covered with a thin layer of water. (a) Power line #1. (b) Power line #2. (c) Power line #3. (d) Power line #4.

from each period of the power line surfaces. At millimeter-wave frequencies where $d > \lambda$, the periodic structure produces significant backscatter at

$$\theta_n = \sin^{-1}\left(\frac{n\lambda}{2L}\right) \tag{1}$$

where λ is the wavelength and L is the period. The measurements show that the Bragg scattering ceases to exist at incident angles larger than 15°. This corresponds to incidence angles beyond which specular points on the power line surface disappear [3]. But, there are still considerable copolarized and cross-polarized backscatter for power lines #2, #3, and #4 at incidence angles larger than 15°. This is attributed to the fact that power line #1 is geometrically more accurate than the others since the number of constituent strands are far fewer than the rest and the copper strands are very tightly wound together. The strands of the outer layer of power lines #2–#4 are aluminum and are somewhat loose, creating a quasi-periodic surface. The degree of disorder increases with the increase in the number of strands and, therefore, the backscatter level of power line #4 at high-incidence angles is higher than the others. This is also demonstrated using a numerical analysis [10]. Important characteristics of power line backscatter behavior are summarized as follows. At the off-specular angles, σ_{vv} is much stronger than the backscatter at other polarizations and increases with increasing the cable diameter D and strand diameter d. At Bragg directions, copolarized backscatters are much stronger than the cross-polarized component, however, at higher incidence the cross-polarized component is stronger than σ_{hh} and weaker than σ_{vv}. The dominance of σ_{vv} at large incidence angles may be attributed to the almost horizontal grooves on the surface of power lines. It is shown that TE electromagnetic waves (in this case, vertical polarizations) can couple into the horizontal grooves (a TEM wave is formed in the groove), whereas for a TM wave (horizontal polarization), the grooves behave as waveguides operating below cutoff [8]. For the most part, the copolarized RCS can be attributed to single reflection from the power line surface. On the other hand, the cross-polarized component is predominantly generated by the multiple reflections from the adjacent strands. Basically, the grooves on the power line surface support dihedral-type double reflections. It is known that tilted dihedrals can generate strong cross-polarized backscatter [11].

The polarimetric backscatter responses of the power lines were also measured under wet condition to investigate the effect of a water layer on the power lines. To maintain the wetness condition throughout the RCS measurements, the power lines were sprayed with water frequently. The backscatter of the wet and dry power lines at vertical polarization are compared in Fig. 4(a)–(d). The results show that for the thin power line, the RCS is increased at high-incidence angles when the surface is made wet and for other power lines the RCS decreased slightly. Similar results were obtained for other polarizations as well. It was also noticed that when the cracks between the wire strands are filled with water, the backscatter RCS is reduced considerably. The latter case can only happen under continuous and relatively heavy rain as the power line structures cannot retain the water.

To complete the experimental aspects of the radar phenomenology of power lines, polarimetric backscatter mea-

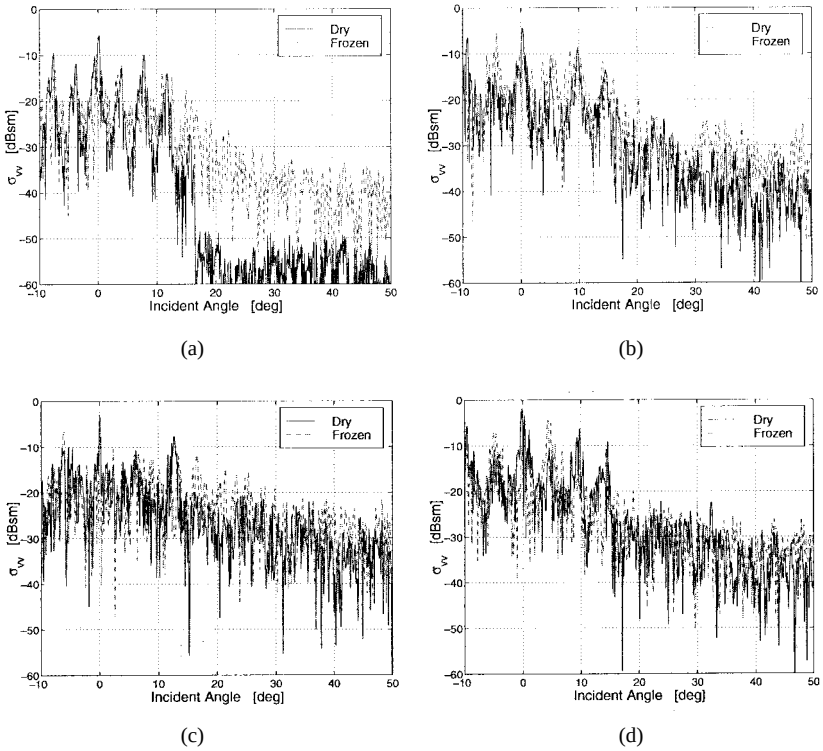

Fig. 5. VV-polarized backscatter responses of the four power line samples covered with a layer of 1-mm-thick ice. (a) Power line #1. (b) Power line #2. (c) Power line #3. (d) Power line #4.

surements of the samples covered with a layer of ice were also performed. The radar and target positioner were set up outdoors on a very cold day. The surface of the power lines were sprayed with water and left to freeze. A layer of ice with an average thickness of about 1 mm was formed on the surface of the lines. Due to gravitational force on dripping water, some short icicles were also formed on the lower surface of horizontal power line samples. Fig. 7 shows the picture of an ice-covered power line used in the backscatter measurements. It is found from the measured results that the RCS of ice-covered power lines are slightly lower than the RCS of dry power lines at angles close to normal incidence (less than 15°), but the RCS increased for higher angles of incidence, as shown in Fig. 5(a)–(d). This behavior was observed for all the power line samples and for all polarization configurations (VV, VH, and HH). In general, water and ice layers modify the RCS by modifying the surface reflectivity and effective surface roughness. As mentioned before, a layer of ice or water lowers the RCS level by few decibels for low incidence angles and increases the RCS level at high-incidence angles. Hence, it can be concluded that the probability of detection is not significantly affected when the cable is covered with a layer of water or ice.

As will be discussed in the next section, the proposed detection algorithm relies on the coherence between copolarized and cross-polarized backscatter of power lines. For ideal situations, that is, perfect power line structure and fixed incident angle, the backscatter is deterministic and, therefore, the copolarized and cross-polarized backscatter are perfectly correlated. However, in practice, there are imperfections in the structure and slight variations in incidence angle due to the radar antenna pattern. Hence, it is important to examine the coherence between copolarized and cross-polarized backscatter by measuring the polarimetric backscatter statistics. The backscatter statistics are generated by moving a relatively small footprint (about 30 cm) over a long piece of power line and rotating the power line about its axis while keeping the aspect angle almost constant. Histograms are generated from 50 independent measurements and six different aspect angles. The phase and magnitude of the copolarized and cross-polarized backscatter at 30° incidence are shown in Fig. 6(a) and (b). Although there are fluctuations in the magnitude and phase of σ_{vv} and σ_{vh}, the fluctuations are almost perfectly correlated. The histograms of the magnitude and phase of $S_{vv}S_{vh}^{*}$ are also shown in Fig. 6(c) and (d).

IV. Detection Algorithm

Detection of power lines using a conventional W-band radar seems only possible over narrow aspect angles where Bragg modes exist. In this situation, there may be enough signal-to-clutter ratio for detecting power line. However, at angles where there exists no strong backscatter from the power line signal-to-clutter ratio is very low and conventional radar systems would fail to detect power lines. In practice, the backscatter from background vegetation or rough surfaces within the same range as the power line may drastically exceed the backscatter from the power line itself. This was the reason for abandoning the idea of using conventional nonpolarimetric millimeter wave radars for power line detection. To circumvent this difficulty, we resorted to radar polarimetry and a statistical detection algorithm for improving the signal-to-clutter ratio.

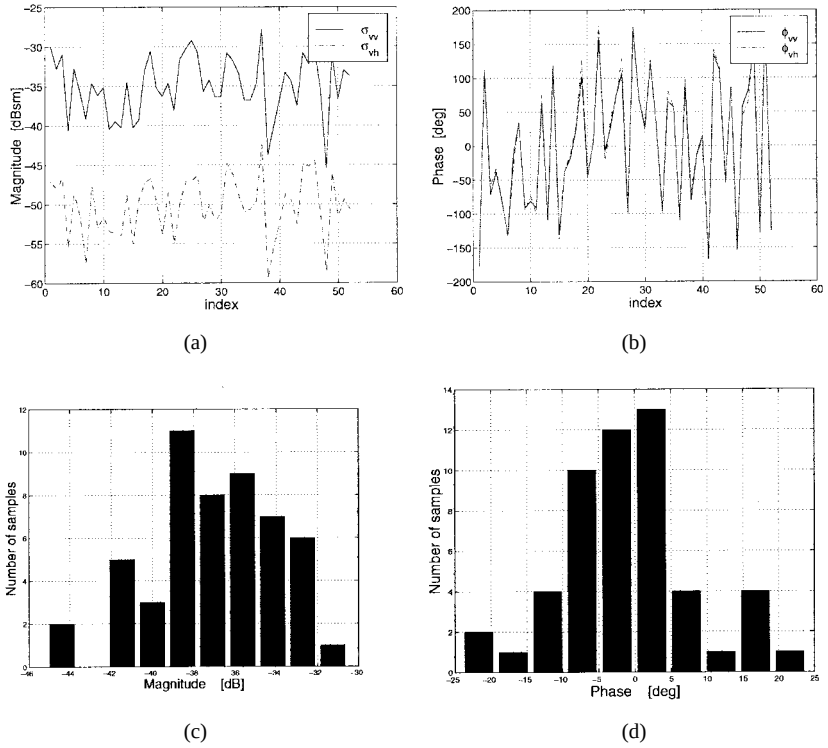

Fig. 6. Coherence test of a power line #4 at incident angle 30°. (a) Magnitude and (b) phase fluctuations as a function of independent measurements for VV and VH backscatter. Also shown is the (c) magnitude and (d) phase of $S_{vv}S_{vh}^{*}$.

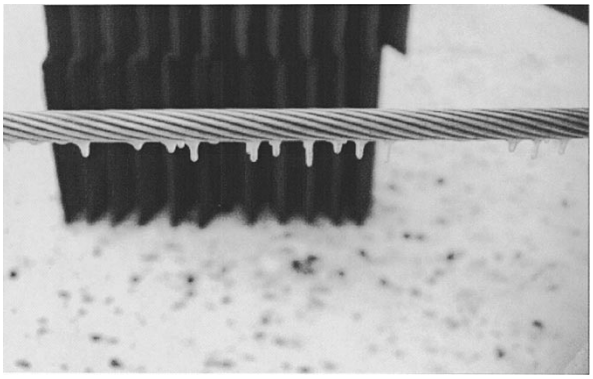

Fig. 7. A picture of power line #2 covered with a layer of ice (thickness ≈ 1 mm) during the backscatter measurements.

Fig. 8. Power line #4 in a background clutter (Douglas fur tree).

Theoretical and experimental investigations show that the copolarized and cross-polarized component of backscatter of distributed targets with azimuthal symmetry are statistically uncorrelated [6]. In other words, $\langle S_{vv}S_{vh}^{*}\rangle$ and $\langle S_{hh}S_{vh}^{*}\rangle$ vanishes for almost all distributed targets provided that footprint is much larger than the field correlation length in the random medium. However, as shown in the previous section, for power lines $\langle S_{vv}S_{vh}^{*}\rangle$ does not vanish. Measuring $\langle S_{vv}S_{vh}^{*}\rangle$ instead of $\langle S_{vv}S_{vv}^{*}\rangle$, for example, should improve detection probability drastically. For example if a radar with sufficient fine range resolution is used, then for any given direction a relatively large number of independent backscatter measurements can be gathered that would allow for estimating $\langle S_{vv}S_{vh}^{*}\rangle$.

Radar backscatter of power lines in the presence of a distributed target whose backscatter is much higher than that of the power line alone were measured and the algorithm was applied to the gathered data for four different aspect angles. Two distributed targets were chosen. One was a Douglas fur tree and the other was an asphalt surface (see Fig. 8). The statistics of the RCS of the distributed targets alone were obtained by rotating the targets. The statistics of the RCS of the power lines with a clutter background were obtained by positioning the power line at a desired aspect angle on a fixed platform and rotating the distributed target (see Fig. 9). For the incident angles which are larger than 20°, RCS of the clutter was found to be much larger than that of the power line alone. For these situations, any conventional detection algorithm fails to detect the power line. Ensemble averaging was achieved by rotating the distributed target (121 angles) and using frequency

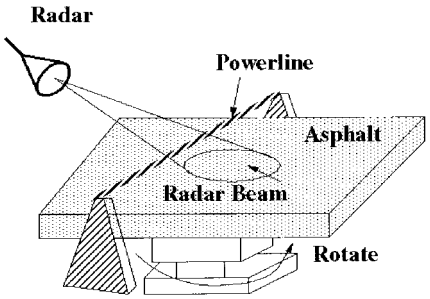

Fig. 9. Measurement setup for power line with asphalt as background clutter.

TABLE II
BACKSCATTER POWER IN CONVENTIONAL CHANNELS AND THE ENSEMBLE AVERAGES OF COPOLARIZED AND CROSS-POLARIZED RESPONSE OF A DOUGLAS FUR TREE AND POWER LINE #4

	$\langle S_{vv}S_{vv}^*\rangle$	$\langle S_{vv}S_{vh}^*\rangle$	$\langle S_{vh}S_{vh}^*\rangle$	$\langle S_{hh}S_{hh}^*\rangle$
Tree alone	−20.6	−42.3	−27.5	−21.2
Tree & power line(0 deg)	−2.4	−8.7	−14.7	−17.4
Tree & power line(10 deg)	−8.7	−16.6	−23.3	−12.3
Tree & power line(20 deg)	−21.0	−30.1	−29.9	−23.1
Tree & power line(30 deg)	−22.2	−31.5	−29.9	−23.1

TABLE III
BACKSCATTER POWER IN CONVENTIONAL CHANNELS AND THE ENSEMBLE AVERAGES OF COPOLARIZED AND CROSS-POLARIZED RESPONSE OF ASPHALT AND POWER LINE #4

	$\langle S_{vv}S_{vv}^*\rangle$	$\langle S_{vv}S_{vh}^*\rangle$	$\langle S_{vh}S_{vh}^*\rangle$	$\langle S_{hh}S_{hh}^*\rangle$
Asphalt alone	−29.8	−43.0	−36.5	−32.9
Asphalt & power line(20 deg)	−25.1	−32.6	−34.3	−33.3
Asphalt & power line(30 deg)	−27.8	−35.6	−35.2	−33.4
Asphalt & power line(40 deg)	−29.4	−36.6	−35.8	−33.7

decorrelation of backscatter response over a 1-GHz bandwidth used in these experiments. Fig. 9 shows the measurement setup used to generate the statistics of the backscatter response of the distributed target and the power line. Table II shows the backscatter power for three conventional polarizations (σ_{vv}, σ_{vh}, σ_{hh}) and the correlation between VV and VH of the tree alone and the tree plus the power line at four different aspect angles. The first two angles were chosen along the Bragg directions where there are significant backscatter and the other two angles were chosen where there are weak backscatter from the power line itself. It is obvious that along the Bragg directions, the power line can easily be detected. However, at other angles the backscatter in conventional channels are far below the clutter (signal-to-clutter ratio < -10 dB). The ensemble average of the cross product for the distributed target alone is of the order of -43 dB whereas $\langle S_{vv}S_{vh}^*\rangle$ for the power line and the tree is around -31 dB, which is 12 dB higher than the tree alone. Similar results were obtained when a rough asphalt surface was used as the clutter and the results are shown in Table III.

V. CONCLUSIONS

Polarimetric radar backscatter measurements of typical power line samples were performed and the effect of braiding on the backscatter response was investigated. The effects of a layer of water or ice on the polarimetric backscatter response were also investigated. It was shown that significant Bragg backscatter exists only for incidence angles below 15°. It was also shown that considerable backscatter exist in VV and VH channels at larger incidence angles which is mostly generated by the geometrical imperfections of power line structures. Based on the observed behavior of the polarimetric backscatter responses, a polarimetric detection algorithm was developed using the existence of correlation between VV and VH backscatter from power lines. The validity of the algorithm for detecting power lines in a strong clutter background was demonstrated under laboratory conditions. The result indicates that for sufficiently large number of independent samples, it is possible to improve the signal-to-clutter ratio by a factor of 20 dB.

REFERENCES

[1] K. Sarabandi, L. Pierce, Y. Oh, and F. T. Ulaby, "Power lines: Radar measurements and detection algorithm for SAR images," *IEEE Trans. Aerosp. Electron. Syst.*, vol. 30, pp. 632–643, Apr. 1994.
[2] A. Nashashibi, K. Sarabandi, and F. T. Ulaby, "A calibration technique for polarimetric coherent-on-receive radar system," *IEEE Trans. Antennas Propagat.*, vol. 43, pp. 396–404, Apr. 1995.
[3] H. H. Al-Khatib, "Laser and millimeter-wave backscatter of transmission cables," *SPIE Phys. Technol. Coherent Infrared Radar*, vol. 300, pp. 212–229, 1981.
[4] B. Rembold, H. G. Wippich, M. Bischoff, and W. F. X. Frank, "A MM-wave collision warning sensor for helicopters," *Proc. Military Microwave*, pp. 344–351, 1982.
[5] M. Savan and D. N. Barr, "Reflectance of wires and cables at 10. 6 micrometer," *Center for Night Vision and Electro-Optics*, MSEL-NV-TR-0063, Jan. 1988.
[6] F. T. Ulaby and C. Elachi, *Radar Polarimetry for Geoscience Applications*. Dedham MA: Artech House, 1990.
[7] Y. Kuga, K. Sarabandi, A. Nashashibi, F. T. Ulaby, and R. Austin, "Millimeter-wave polarimetric scatterometer systems: Measurement and calibration techniques," *Proc. AGARD 48th Symp. Electromagn. Wave Propagat. Panel*, Montreal, Canada, May 1991, pp. 28-1–28-5.
[8] T. B. A. Senior, K. Sarabandi, and J. Natzke, "Scattering by a narrow gap," *IEEE Trans. Antennas Propagat.*, 38, pp. 1102–1110, July 1990.
[9] J. B. Keiler, "Diffraction by a convex cylinder," *IRE Trans. Antennas Propagation*, vol. AP-4, p. 312, 1956.
[10] M. Park and K. Sarabandi, "Millimeter-wave scattering from high voltage power lines: A second-order physical optics model," *IEEE Trans. Antennas Propagat.*, to be published.
[11] W. C. Anderson, "Consequences of nonorthogonality on the scattering properties of dihedral reflectors," *IEEE Trans. Antennas Propagat.*, vol. AP-35, pp. 1154–1159, Oct. 1987.

Kamal Sarabandi (S'87–M'90–SM'92–F'00), for photograph and biography, see p. 861 of the May 1999 issue of this TRANSACTIONS.

Moonsoo Park was born in Seoul, South Korea, on February 4, 1964. He received the B.S. and M.S. degrees in electronics engineering from Seoul National University, Seoul, South Korea, in 1987 and 1989, respectively. He is currently working toward the Ph.D. degree in electrical engineering at the University of Michigan, Ann Arbor.

From 1989 to 1993, he worked as an RF/Microwave Design Engineer in Daewoo Electronics, Seoul, South Korea. He is currently a Research Assistant with the Radiation Laboratory, the University of Michigan, Ann Arbor. His research interests include polarimetric millimeter-wave radar systems for navigations, millimeter-wave remote sensing, wave scattering, and SAR image processing.